

Flow Distribution Measurements at the Exit of Bipolar Plates in a PEM Fuel Cell Stack by a Scanning Light Sheet Method

Messung der Strömungsverteilung am Austritt von Bipolarplatten in einer Brennstoffzelle durch Lichtschnitt-Abtastung

J. Klinner¹, C. Willert¹, A. Schneider², A. Mack-Gardner²

¹ DLR – Deutsches Zentrum für Luft- und Raumfahrt e.V., Institut für Antriebstechnik, Linder Höhe, 51147 Köln, email: joachim.klinner@dlr.de

² Adam Opel GmbH, GM Alternative Propulsion Center Europe, IPC MK-01, 65423 Rüsselsheim

PIV, miniaturized light sheet probe, PEMFC, fuel cell stack, bipolar plates, flow distribution
PIV, Lichtschnittsonde, Brennstoffzelle, Bipolarplatte, Strömungsverteilung

Abstract

This paper summarizes two different experimental approaches which concentrate on capturing the exit flow distribution of the anode side of a prototype fuel cell stack operated with air at realistic flow rates. The first approach intends to visualize the penetration depth of the millimetre-sized exit jets in a laminar mixing flow by introducing oil-based tracer particles to the exit header and leaving the bipolar plates and exit jets unseeded. The second approach concentrates on measuring the exit jet velocity field downstream of the channel exits by particle image velocimetry (PIV) and by applying a water-based micron-sized droplet seeding to the bipolar plate channels. The traversal of the imaged plane along the bipolar plate exits finally allowed the reconstruction of the complete three-dimensional, time-averaged flow field in high resolution (restricted to two components of velocity). An overview of the experimental setup, including the implementation of a miniaturized light sheet probe, and the data evaluation are given. In addition, the application of a robust PIV evaluation algorithm based on multi-grid, multi-pass correlation averaging methods is described which had to be applied at higher flow rates due to highly dynamic fluctuations of the flow, lower particle image density and regionally significant background signal due to laser flare on the stack plates.

Introduction

The performance of proton exchange membrane fuel cells (PEMFC) strongly depends on a homogeneous distribution of hydrogen and oxygen along the bipolar plate channels preferably under richer-than-stoichiometric conditions. Further, a uniform flow distribution along the cells of a stack is critical in order to obtain high efficiency. Cell-to-cell variation can occur due to varying manufacturing parameters and, for instance, by the intrusion of the porous gas diffusion layer (GDL) into the channels due to varying compression [Owejan et al 2009]. Therefore it is necessary to experimentally verify the uniformity of the flow distribution in a representative complete stack assembly. This would also include effects of uneven local pressure distribution in the inlet and exit manifolds caused by the specific placement of the inlet/outlet pipes and manufacturing tolerances causing uneven flow resistance in the bipolar plates [Chang et al 2006, Kandlikar et al 2009]. These effects can be studied by measuring the spatially resolved flow field immediately downstream of the bipolar plate channel exits.

Two different experimental approaches have been carried out that concentrate on the flow field of the anode side of a prototype PEMFC stack. The first approach is based on capturing Mie-scattering of tracer particles which are added to the exit header, leaving the bipolar plates and exit jets unseeded. The laminar mixing flow of dry air coming from the channel exits and from seeded header flow is observed by the camera while tracer particles are illuminated by a continuous-wave laser light sheet. The technique intends to visualize the penetration depth of the millimetre-sized exit jets and is based on principles of the Quantitative Light Sheet Scattering method (QLS) which is described in [Voigt 1996, Röhle et al 2000, Findeisen et al 2005]. On the other hand the PIV approach is able to measure the averaged exit jet velocity field downstream of the channel exits in the entire stack. Different operation points of the stack from minimum flow rate up to a 30 times higher flow rate have been investigated by PIV. In this operating regime the flow at the channel exits is in transition from laminar to turbulent.

Both methods made use of a miniaturized light sheet probe which generates a 3 mm wide light sheet along the exit channels and can successively be positioned at different bipolar plate levels inside of the exit manifold. The optical probe design criterions had to meet several conditions such as ensuring a light sheet thickness below the channel height and maintaining a constant light sheet alignment while traversing across the stack height.

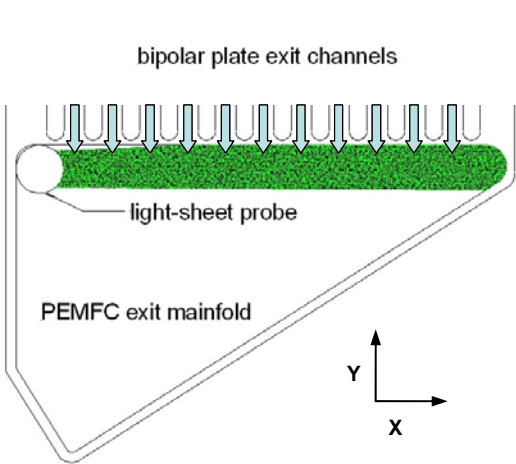


Fig. 1 Light sheet orientation inside the exit manifold, bipolar plate geometry from Thompson et al 2007

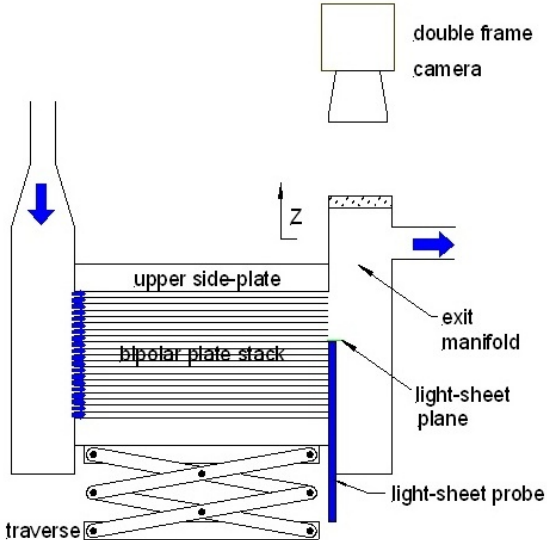


Fig. 2 Measurement setup

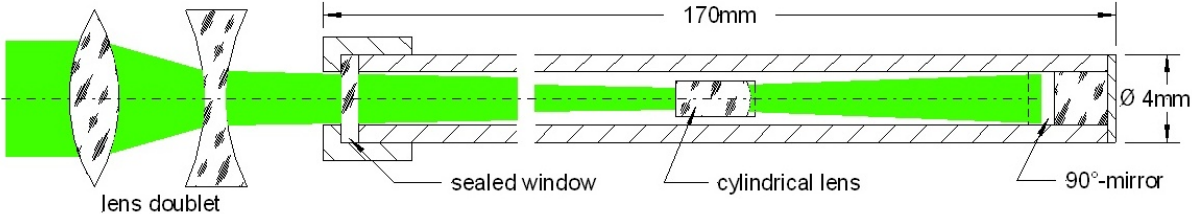


Fig. 3 Light sheet probe

Experimental setup

The light sheet was oriented along bipolar-plate exits and had to scan over 29 mm stack height on z-axis. This was implemented by traversing the stack with respect to a laboratory fixed light sheet probe and camera (Fig 2). The step-and-repeat positioning accuracy of the fuel cell was verified by an indicating calliper and is about $\pm 4 \mu\text{m}$. The z-axis of the stepper points toward the camera and the upper side plate of the stack had been aligned parallel along the x-y-plane. The x-axis of the measurement coordinate system was oriented along the rim of the upper bipolar plate (Fig 1). The stack exit was sampled at up to 150 planes using traverse increments of 0.2 mm which roughly corresponds to 5 planes per bipolar-plate.

The light sheet probe (Fig 3) was introduced in the anode exit header through a slide bearing. Certain optical components had to be installed in a 170 mm long VA-tube with 3 mm free aperture. A tailored rectangular cylindrical lens was fixed in a wire-eroded $3 \times 2 \text{ mm}^2$ radial-oriented cut-out of the tube. The 90° -mirror was coated on a 45° chamfered 3 mm diameter BK7-glass rod which was glued on the probe tip. The laser-beam diameter was narrowed onto inner tube diameter by a lens doublet. This doublet was also used to focus the light sheet waist through the tube at an overall distance of 210 mm.

Because of best accessibility and least occurrence of laser light reflexions the upper left corner of the triangle-shaped exit header was chosen for the probe position. Bearing, laser probe and laser beam were aligned coaxial to minimize change of light-sheet position during a scan. Residual misalignment due to non-concentricity of the probe-tube (maximum free-standing length during a scan 120 mm) could be evaluated by observing the probes end tip with the camera and was approximately $\pm 0.2 \text{ mm}$ in the x-y-direction during one scan.

Images were captured through a high-quality glass window installed above the exit header. For image acquisition a PCO1600 at 1600×256 pixel resolution equipped with a macro-lens ($f = 100 \text{ mm}$) was used at a magnification of 41 px/mm.

For initially applied visualisation technique light sheet illumination was realized by a continuous-wave and frequency-doubled DPSS Nd:Yag laser at 300 mW. An additional access port was installed in the exit header where seeded air was fed in at twice the flow rate compared to anode flow. Seeding consisted of paraffin oil droplets dispersed by an atomizer. The camera observed the mixing flow between clean and seeded air at a given light sheet position. Exposure times as short as 5 ms could be reached for this setup which was sufficiently short not to blur images of the exit jets at low flow rates.

For PIV experiments a flash lamp pumped double-pulse Nd:YAG laser at 15 Hz repetition rate was used. Pulse energy was attenuated down to 1.5 mJ which was sufficient to illuminate water droplets in the $33 \times 3 \text{ mm}^2$ field of view. In order to focus the light sheet waist through the 170 mm long probe at a free aperture of 3 mm the divergence had to be limited to 7.5 mrad. The light sheet thickness increases at low divergence angles, especially for flash lamp pumped lasers with M^2 -factor larger than 1. In addition, light sheet thickness had to be kept below channel exit height in order not to under-sample the narrow exit jets. To verify these criterions sheet thickness was evaluated by a beam profiler. Laser intensity was recorded at different x-positions and fitted along z by a least-square gauss fit. Within viewing area the sheet thickness was found to be below 0.2 mm at $1/e$ intensity level.

The proton exchange membrane of bipolar channels has a hydrophilic character and would be irreversibly damaged by applying hydrophobic oil-based seeding. Therefore a water-based droplet seeding consisting of a mixture of water and 5% Polyethylene-glycol (PEG) was applied. The latter was used to reduce the evaporation rate of the micron-sized water droplets. The aerosol seeding droplets were created following an atomization principle suggested by Laskin [Raffel et al 2007]. A separator and a large reservoir upstream of the fuel stack inlet removed larger droplets.

Results of Visualisation

At low flow rates (approx. 7-10 slm) the signature of the exit jets in seeded air could clearly be visualized only at positions where the strong laminar character of both flows is preserved (Fig. 4). Conclusions about penetration depth of the exit jets are possible at these regions only. Mixing of both flows reduces contrast and occurs in the right corner of the exit header due to the narrow geometry (right hand side in Fig. 4). Flow can only be visualized in the presence of seeded and unseeded air in the viewing area. For these reasons this method could only be applied at lower regions of the stack where the seeded air flows in close proximity of the exit channels. At positions closer to the stack outlet the seeded air is more and more blocked by clean air coming from channel exits of the lower areas of the stack. Therefore this technique was not further developed and in a secondary step PIV was applied to capture the flow distribution of the entire stack.

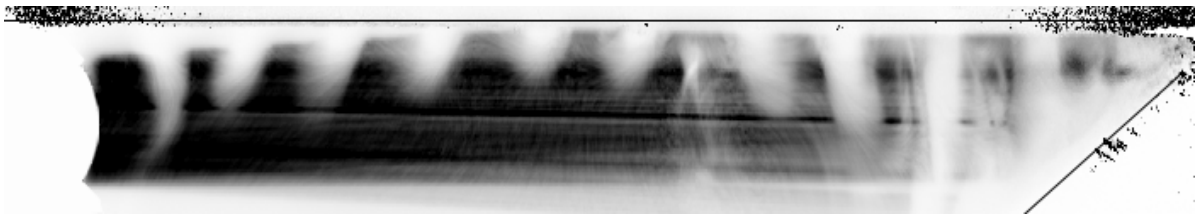


Fig. 4 Visualization of exit channel flow of a bipolar plate, light sheet probe is implied on left hand side, unseeded regions of exit jets are bright (negative image)

PIV data acquisition and evaluation

For PIV measurements the stack was only supplied with seeded air from the settling chamber for the duration of the PIV image acquisition (approx. 27-35 s/pos). The remainder of the time, that is image read-out and traversal to the next position, the stack was purged with clean air (90 s/pos) in order to keep water droplet deposition inside the channels at an acceptable level. A measurement cycle at a given position consisting of image recording and subsequent image storage took on the order of 2 minutes. A scan of the average flow distribution of the entire stack included PIV measurements at 150 planes successively and therefore took about 5 hours. Differential pressure between inlet and exit header was monitored during entire scan.

While the differential pressure remained constant during tests at minimum flow rate (approx. 7 slm), it continuously increased up to 26% during the 5 hour scan at maximum flow rate (approx. 210 slm). Most likely this is due to residual water droplets collecting on the inner surfaces of the fuel cell gas channels.

Afterward the stack was dried by purging with air. Due to this differential pressure is reduced to the initial level. Repeated flow measurements in the dry stack at similar mass flow showed no influence on the velocity field.

Because of different experimental conditions at minimum flow rate and at maximum flow rate two different evaluation schemes had to be used. At minimum flow rate the entire gas flow could be directed through the Laskin particle generator and therefore be enriched by water droplets. Because of no further dilution a maximum droplet density could be reached. After suitable image contrast enhancement by minimum background subtraction each PIV double image could be evaluated using a coarse-to-fine multi-grid processing scheme. The sub-pixel correlation peak position measurement was performed by a truncated sinc signal reconstruction algorithm. Due to this processing and a sufficient particle image density an accuracy of correlation peak detection below ± 0.1 pixel can be obtained for regions without strong laser background [Raffel et al 2007]. The latter occur where the laser light hits bipolar plates or

PEM sheets partially sticking out of the stack. This can lead to incorrect correlation peak detection due to low signal-to-noise ratio. To exclude these outliers from averaging or to replace them by lower-order correlation peaks a maximum displacement difference and a normalized median validation was applied.

At the highest flow rate only 38% of gas flow could be directed through the Laskin particle generator and therefore be enriched by water droplets. In addition, water droplet deposition may have occurred due to higher gas velocity in the channels. This was confirmed by the previously mentioned gradually increasing differential pressure between inlet and exit header. For these reasons particle image density was significantly lower compared to images at minimum flow rate. A reliable validation of single-image evaluations was not possible because of the turbulent nature of the flow. Hence the averaging of velocities coming from single-image evaluation led to underestimated jet exit velocities. Artifacts such as velocity gradients along the light sheet border (in y-direction) were observed.

The data quality could be improved by applying a new multipass ensemble correlation [Willert 2008]. Here the averaging of correlation planes for a sequence of images is combined with an iterative offsetting of interrogation windows according to mean displacement. On the one hand signal enhancement due to accumulation of single correlation peak can be obtained, and, on the other hand, the fraction of matched particle images is increased. Therefore signal-to-noise ratio of the correlation signal-peak is improved significantly.

Results of PIV measurements

At minimum flow rate 200 images have been averaged at each of the 150 sampling positions. The Reynolds number of the exit jets is about 10-20 (based on the mean jet velocity and the width of the exit channels). Single exit jets can clearly be identified. Laminar character is also confirmed by a convergence test of the RMS values of the main jet velocity which are constant within a ± 0.004 m/s margin already after 100 averaged measurements.

At maximum flow rate Reynolds number of the header exit jets is about 2000 and in transition to turbulent flow. Due to the stronger exit flow impulse recirculation regions can clearly be identified (Fig. 4). Instantaneous PIV evaluations show single jets and their recirculation appearing and disappearing at different exits during data acquisition at one light sheet position. After averaging over 300 available images the v-velocity decreases significantly due to this effect. Some of the exit jets still show velocity gradients along y. One possible explanation for this might be that not all channels deliver constant particle rates. In these cases the signal is provided by surrounding particles that are entrained by the jet and obviously have velocities below the true jet velocity.

Conclusions

Within the presented work it was shown that particle image velocimetry is a suitable tool for mapping of the gas flow distribution within the exit header of a fully assembled fuel cell. The application of a miniaturized light sheet probe in combination with a scanning light sheet approach allowed the capture of the average velocity flow field of the entire stack at 150 planes during a 5 hours run at a z-resolution of 0.2 mm. The application of a water-based droplet seeding on anode channels allowed stable particle rates during the entire scan. Still there is room for improvement regarding particle image rates at maximum flow rate of the prototype PEMFC. The quality of the averaged PIV results at high flow rates could significantly be improved by applying a multipass ensemble correlation technique.

The initially applied visualization technique could not deliver the flow distribution in the entire stack due to blocking of seeded air. Nonetheless, this technique is attractive because bipolar plates are left unseeded and might be applied for small stack assemblies.

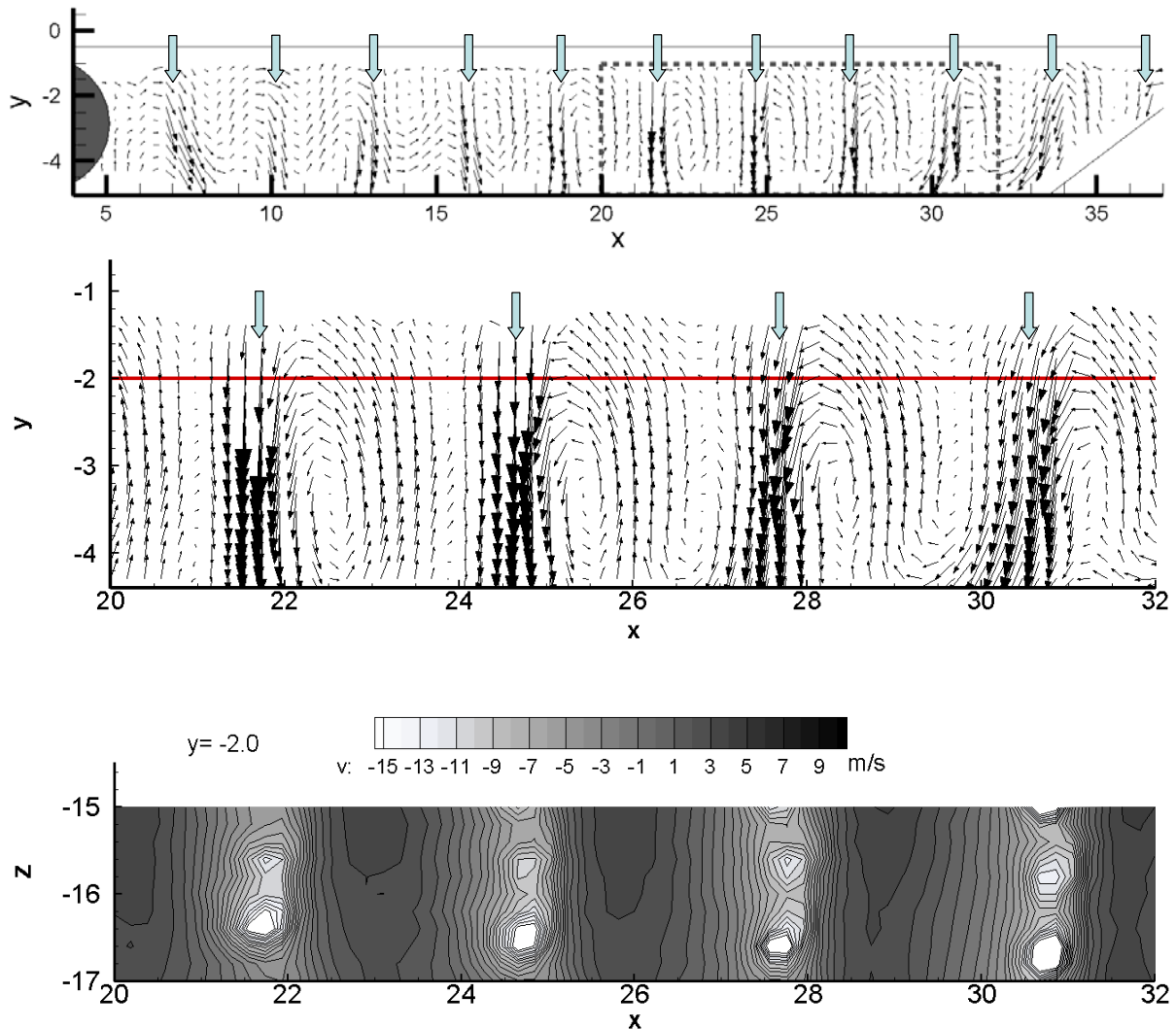


Fig. 5 Exemplary result of average velocity field at maximum flow rate, top: overview of averaged planar flow field at one light-sheet position, middle: section of x-y flow field, bottom: v-component in x-z at y=-2 mm, result was interpolated by inverse distance method, net-points distances are 0.2mm in z, 0.19 mm in x,y

References

Paul A.C. Chang, Jean St-Pierre, Jürgen Stumper, Brian Wetton, 2006: Flow distribution in proton exchange membrane fuel cell stacks. *Journal of Power Sources*, Volume 162, Issue 1, November 8 2006, Pages 340-355

J. Findeisen, M. Gnirß, N. Damaschke, H.-P. Schiffer, C. Tropea, 2D – Concentration Measurements Based on Mie Scattering using a Commercial PIV system. In: 6th International Symposium on Particle Image Velocimetry Pasadena, California, USA, September 21-23, 2005

S.G. Kandlikar, Z. Lu, W.E. Domigan, A.D. White, M.W. Benedict, Measurement of flow maldistribution in parallel channels and its application to ex-situ and in-situ experiments in PEMFC water manage-

ment studies, International Journal of Heat and Mass Transfer, Volume 52, Issues 7-8, March 2009, Pages 1741-1752

Jon P. Owejan, Jeffrey J. Gagliardo, Jacqueline M. Sergi, Satish G. Kandlikar, Thomas A. Trabold, 2009: Water management studies in PEM fuel cells, Part I: Fuel cell design and in-situ water distributions. International Journal of Hydrogen Energy, Volume 34, Issue 8, May 2009, Pages 3436-3444

M. Raffel, C. Willert, S. Wereley, J. Kompenhans, 2007: Particle Image Velocimetry – A Practical Guide. 2nd Edition, Springer Verlag

I. Röhle, R. Schodl, P. Voigt, C. Willert, 2000: Recent developments and applications of quantitative laser light sheet measuring techniques in turbomachinery components. Measurement, Science & Technology , 11 (7) , Pages 1023-1035

Eric L. Thompson, Steven G. Goebel, Scott Ofslager, 2007: Verbesserte Strömungsfeldplatten. Patent DE 11205003052T5

P. Voigt, 1998: Non-linear effects in planar scattering techniques: proof of existence, simulations and numerical corrections of extinction and multiple scattering. Proc. 9th Intl. Symp. on Applic. of Laser Techniques to Fluid Mechanics, Lisbon (Portugal), 13-16 July

C. Willert, 2008: Adaptive PIV Processing Based on Ensemble Correlation. Proc. 14th Intl. Symp. on Applic. of Laser Techniques to Fluid Mechanics, Lisbon (Portugal), 7-10 July